Proceedings of the 5th International Symposium on Future Active Safety Technology toward Zero Accidents
(FAST-zero '19)
September 9-11, 2019, Blacksburg, VA, USA

Behaviour investigation of a risk-aware driving model for trajectory prediction

Fabian Müller and Julian Eggert

Landgraf-Georg-Str. 4
Darmstadt, D-64283, Germany
Phone: +49 (0) 6151 16 25037
E-mail: fabian.mueller@rmr.tu-darmstadt.de
Co-author's E-mail: julian.eggert@honda-ri.de

June 28, 2019

Keyword(s): Risk Assessment, Safety, Trajectory Prediction, Trajectory Planning

Abstract

The prevention of risky situations is one of the main tasks in autonomous driving (AD) and intelligent driving assistant systems (ADAS). Uncertainty in the traffic participants' behavior and the sensor measurements leads to critical situations, which have to be anticipated by appropriate risk prediction approaches. The risk prediction itself requires dedicated driver models which are interaction sensitive and computationally cheap, to efficiently simulate how a scene might evolve. In this paper, we present a new driver model which is aware of the usual risks encountered in normal driving scenarios. It can cope with longitudinal as well as lateral collision risks, and adjusts its behavior by minimizing the expected integral risk. We show how our model is suited for coping with parallel lane scenarios like overtaking, following and in-between positioning by analyzing its behavior and stability.

I. Introduction

The zero accident scenario is a major target for implementing autonomous vehicles on streets. Critical situations, where the scene can evolve into severe accidents, should be avoided. In addition to slippery roads and narrow curves, inter-vehicle collisions are among the main causes for fatal outcomes.
For inter-vehicle collisions, knowledge about the future development is key for acting safely. In a totally deterministic environment, where the future evolution is known, trajectory planning can treat undesired future states as forbidden so that the focus is on efficient and comfortable maneuvers [1]. Uncertainties in sensor measurements and in the execution of maneuvers of traffic participants undermine the hard constraints of forbidden collision states. With this extended consideration, at every future time point the traffic participant has got a potential to end up in a collision.
Risk is defined in [2] as the product of an event probability and the corresponding event severity e.g. the collision probability multiplied by the collision severity. The probability of a collision is usually given by considering the overlap of the vehicle shapes where the vehicle states, like position and velocity, follow probabilistic distributions. The distributions account for the hypothetical evolution of future scenes caused by varying maneuvers as well as for sensory uncertainties. The severity determines the consequences of an event resulting e.g. in traffic participant injuries, damages on vehicle and street objects or economical costs like loss of productivity. Accordingly, in high-velocity scenarios like on highways, the consequences of a fatal crash by accident is higher than for low velocity in residential areas.
Risk assessment approaches try to warn human drivers in critical situations by analyzing the entire scene, so that the driver is able to adapt its behavior to relax situations in terms of criticality [3, 4]. To drive autonomously, the human driver is replaced by a system which adapts its behavior to the current scene risk, with a motion planner that seeks a trade-off between minimizing risk while maximizing traveling benefit. For this purpose, [5] predicts trajectory candidates and evaluates their overall cost in terms of risks and benefits. In other work [6], the overall risk is approximated by taking only the point of maximum risk into account to adapt the behavior of the planner.

License: CC BY 4.0 International - Creative Commons, Attribution

In this paper, we start from [6] as a model for driving behavior and analyze the capabilities of the approach for reproducing human-like behavior. We show how a motion planner based on a grounded risk approach, incorporating probability and severity models, can incorporate many risk sources into its decision making, which leads to known macroscopic behavior in parallel lane scenarios. In detail, we show how our planner avoids collision, can stick approximately to the two-seconds headway distance rule [7] in following scenarios, decreases continuously its longitudinal stability distance to the frontal vehicle from a non-overtaking to an overtaking scenario and decreases autonomously its velocity depending on the lateral distance during overtaking. Furthermore, we investigate how our model is able to position itself between two vehicles in an in-between-following scenario depending on the available gap size.

II. Risk-based Planner

The task of a motion planner is to estimate safe trajectories. For this purpose, for every traffic participant, we predict their future states, like position and velocity along given spatial paths. We combine all states at one current or future time point into one world state $\vec{x}(t) = [\vec{x}_0(t), \vec{x}_1(t), ..., \vec{x}_{\text{Np-1}}(t)]^T$, where the index 0 stands for our **Ego** vehicle and the remaining $N_\text{p} - 1$ indices belong to **Other** participants. Each vehicle motion is modeled by a discrete double integrator system $\vec{f}_\text{i}$ with acceleration as input: $\vec{x}_\text{i}(t+\Delta t) = \vec{f}_\text{i}(\vec{x}_\text{i}(t), a_\text{i}(t))$. The ego acceleration $a_0(t)$ is restricted by a maximum a_max and a minimum while braking a_min, which has to be considered by our planner. The Other traffic participants are modeled with constant velocity like in [3]. With the knowledge about future inputs $a_\text{i}(t+s)$ for all $s > 0$, we can predict the future world states.
In the first subsection (*A.*), we will introduce the used risk model with its subcomponents and explain how different risk sources can be combined to one accumulated risk value. The main contributions to the risk model will be explained in detail in the two subsequent sections: the collision rate for the probability estimation (*B.*) and the collision severity (*C.*). Based on that, we present the strategy of minimizing the overall predicted costs comprising both risk and utility factors to avoid critical situations and acting efficiently (*D.*).

A. *Risk Model*

We model a risk within a time interval $[t+s, t+s+\Delta t]$ as the probability of a particular event within that time interval multiplied by its severity (see Eq. (1)). The risk value around that specific time point $t+s$ can have multiple causes like collisions with traffic participants, collisions with road infrastructure, or loss of control of the vehicle in curves. Each critical event $e \in \{coll, curve, ...\}$ is modeled by its probability $P_\text{FE,e}$ and its corresponding severity C_e.

$$R_\text{e}(t+s; t, \Delta t) = P_\text{FE,e}(t+s; t, \Delta t) \cdot C_\text{e}(t+s) \tag{1}$$

Here, the first event probability $P_\text{FE,e}$ is the probability of getting involved in an event e at $t+s$ after starting at t *if the Ego-vehicle did not get involved in any critical event before*, i.e. , given its history from t until $t+s$. To arrive at this probability, we first have to consider the probability P_e of a possible critical event at one particular time point in future without considering its history, because events earlier in time reduce the probability of getting involved in any critical event further in time. Therefore it holds that the first event probability can never be higher than the history independent instantaneous probability $P_\text{FE,e}(t+s; t, \Delta t) \leq P_\text{e}(t+s; \Delta t)$. To get the instantaneous probability, we introduce a rate function τ_e^{-1} [8] which determines how many events take place on average per time interval, assuming that the events are stochastic (see Eq. (2)).

$$P_\text{e}(t+s; \Delta t) := \tau_\text{e}^{-1}(t+s)\,\Delta t \tag{2}$$

For each event e, the corresponding rate τ_e^{-1} must be determined. In addition, each event e, which can take place in the same time interval, reduces the probability to reach the next state on the predicted trajectory. For small probabilities it holds that the representative total event rate $\tau_\text{tot}^{-1} = \sum_e \tau_\text{e}^{-1}$, i.e., it is approximately the sum over all single event rates for this time interval.
We introduce a history incorporating survival function $S(t+s, t)$ [8] which indicates the probability of not getting involved in any event until reaching a particular time point $t+s$ to fill in the gap between both above mentioned instantaneous event probabilities (see Eq. (3)).

$$P_\text{FE,e}(t+s; t, \Delta t) = P_\text{e}(t+s; \Delta t)\, \exp\left\{ -\int_0^s \tau_\text{tot}^{-1}(t+s')\, ds' \right\} = P_\text{e}(t+s; \Delta t)\, S(t+s, t) \tag{3}$$

With increasing time it becomes certain that the Ego vehicle does not reach the end of the trajectory. This is also guaranteed by introducing a special event with an escape rate τ_esc^{-1} (and zero severity C_esc=0), which accounts for unexpected behavior deviating from the predicted trajectories. The escape rate ensures that the survival function is

always decreasing with increasing time resp. converges to zero for $s \to \infty$. As a consequence, the survival function weights events earlier in time higher than those further in future.
Finally, to estimate the risk of the entire scene based on given predicted trajectories, the severity $C_{\mathrm{e}}(t+s)$ weights the probability at each time point, so that we integrate the particular risks for one specific event $R_{\mathrm{e}}(t+s;t,\Delta t)$ over the entire future time with Eq.'s (1), (2) and (3) to obtain the following equation for the corresponding integrated risk $R_{\mathrm{INT,e}}$:

$$R_{\mathrm{INT,e}}(t) = \int_0^\infty C_{\mathrm{e}}(t+s)\ \tau_{\mathrm{e}}^{-1}(t+s)\ S(t+s,t)ds \tag{4}$$

In this paper, we are primarily interested in risks generated by collisions with other vehicles, so that we introduce our model for the corresponding collision rate $\tau_{\mathrm{coll}}^{-1}$ in the next section.

B. Collision Rate

The collision rate $\tau_{\mathrm{coll}}^{-1}$ determines the instantaneous, history-free probability density at a particular time point of getting involved in a collision event. To incorporate sensor or behavioral uncertainties for future predictions, the representative trajectories of all traffic participants are Gaussian distributed in their position and velocity. Furthermore, the velocity distribution depends on its current mean velocity: $\sigma_{\mathrm{v}}(t+s) = \alpha_{\mathrm{v}}\hat{v}(t+s)$ with $\hat{v}(t+s) > 0$. With increasing prediction time, the Gaussian positional variances increase, reflecting a larger uncertainty about the vehicle position.

$$[\sigma_{\mathrm{x}}(t,t+s)]^2 = [\sigma_{\mathrm{x}}(t)]^2 + [\sigma_{\mathrm{x,v}}(t+s)]^2 \quad \text{with} \quad \sigma_{\mathrm{x,v}}(t,t+s) = \alpha_{\mathrm{v}}[\hat{x}(t+s) - \hat{x}(t)] \tag{5}$$

The collision rate $\tau_{\mathrm{coll}}^{-1}$ is gained by an indicator function I_{coll} (see (7)). The indicator function I_{coll} describes the probability of a collision between two vehicles, approximated by the spatial overlap of their 2D shapes. In a simplified orthogonal setting, assuming stochastic independence for each time step, we can calculate the distribution of the distance between two traffic participants by convolution resulting in a Gaussian distribution with variance $\sigma_{\mathrm{d,x}}^2 = \sigma_{\mathrm{x,i}}^2 + \sigma_{\mathrm{x,0}}^2$ and mean distance $\hat{d}_{\mathrm{x}} = \hat{x}_{\mathrm{i}} - \hat{x}_0$. The vertical mean distance $\hat{d}_{\mathrm{y}}$ and variance $\sigma_{\mathrm{d,y}}^2$ are calculated in an analogous way. The indicator function is now gained by integrating the positional Gaussian distance distribution over the spatial overlap interval $[-d_{\mathrm{x,min}}, d_{\mathrm{x,min}}] \times [-d_{\mathrm{y,min}}, d_{\mathrm{y,min}}]$, where the integration limits $d_{\mathrm{x/y,min}}$ are given by the width respectively length of the involved vehicles in parallel lane scenarios. This ends up into (6).

$$I_{\mathrm{x/y,\,coll}} = \frac{1}{2}\left(\mathrm{erf}\left[\frac{d_{\mathrm{x/y,min}} - \hat{d}_{\mathrm{x/y}}}{\sqrt{2}\,\sigma_{\mathrm{d,x/y}}}\right] - \mathrm{erf}\left[\frac{-d_{\mathrm{x/y,min}} - \hat{d}_{\mathrm{x/y}}}{\sqrt{2}\,\sigma_{\mathrm{d,x/y}}}\right]\right) \tag{6}$$

$$\tau_{\mathrm{coll}}^{-1}[I_{\mathrm{coll}}] := \tau_{\mathrm{max}}^{-1}\left(1 - e^{-\beta I_{\mathrm{coll}}}\right)\left(1 - e^{-\beta}\right)^{-1} \quad \text{with} \quad I_{\mathrm{coll}} = I_{\mathrm{x,coll}} \cdot I_{\mathrm{y,coll}} \tag{7}$$

The constant τ_{max}^{-1} sets the maximum collision rate and the parameter β represents the slope. With (7) and all other event rates along the trajectory, we can now calculate the survival function with (3). However, to obtain the overall risk in Eq. (4), a suitable model for the related collision severity $C_{\mathrm{coll}}(t+s)$ has to be included., which is going to be introduced in the next section.

C. Collision Severity

The severity $C_{\mathrm{coll}}(t+s)$ quantifies the outcome of a collision by regarding the predicted states of the involved traffic participants at the moment of collision. There are several models used for criticality assessment, which model the outcome produced by the first touch event. E.g. [4] and [9] approximate the collision severity with a constant impact factor. In [10] and [11] the severity depends on the square of the Ego velocity. [12] and [13] model a ball impact with vehicle masses as a basis for a collision impact cost calculation. A physically more complex model for inter-vehicle crashes is presented in [14], where the vehicles are modelled as a simple mass-spring model with stiffness assumptions to determine the forces that affect the passenger when hitting an interior. [15] states that a Maxwell model (serial damper and stiffness) fits best for low velocity frontal barrier crashes.
In this paper, we introduce an alternative severity model which considers the main and one subsequent crash event, the crash dynamics and the monetary costs of injuries.
After the first touch, we assume that a loss of control might occur with subsequent crashes against street objects or walls which increase the severity. Therefore we model the first touch as a normal inter-vehicle collision *v2v* and all subsequent events are combined into a "wall" collision *v2w*.

$$C_{\mathrm{coll}}(t+s) = C_{\mathrm{v2v}}(t+s) + p(\mathrm{v2w}|\mathrm{v2v})\,C_{\mathrm{v2w}}(t+s) \tag{8}$$

Because we do not model the after crash scenario within the scene in detail, we assume a fixed conditional probability $p(\text{v2w}|\text{v2w})$ of getting involved into the "wall" collision.
The total costs of a crash C are given by the sum of different single costs like property damage, economical and medical costs for injury care and hospital stay. We see the medical costs as the dominant factor and use a model which transforms the ego velocity change through crash $\Delta v_{\text{v2v/v2w}}$ into monetary values. The correlation is given by a logistic function for serious occupant injury [16], which can be transformed into monetary values from humanity costs of severe injured persons [17]:

$$C_{\text{v2v/v2w}} = C_{\max} \cdot \left(1 + e^{-a \cdot (|\Delta v_{\text{v2v/v2w}}| - v_{\text{th}})}\right)^{-1}. \tag{9}$$

The parameter $C_{\max}$ defines the maximum severity of a potential crash in terms of money, a the rise and v_{th} the threshold value for the logistic function. To get the velocity change through crash $\Delta v_{\text{v2v/v2w}}$, we take an one-dimensional inelastic ball impact with vehicle masses M_0, M_{i} and use the predicted mean longitudinal velocities $\hat{v}_0(t+s)$ and $\hat{v}_{\text{i}}(t+s)$ of the involved Ego and Other vehicle:

$$\Delta v_{\text{v2w}} = -(1 + r_{\text{v2w}})(\hat{v}_0(t+s) + \Delta v_{\text{v2v}}) \tag{10}$$

$$\Delta v_{\text{v2v}} = \frac{M_{\text{i}}}{M_{\text{i}} + M_0}(1 + r_{\text{v2v}})(\hat{v}_{\text{i}}(t+s) - \hat{v}_0(t+s)). \tag{11}$$

The restitution coefficients $r_{\text{v2w/v2v}}$ indicate the elasticity of the impact and serves to model the energy dissipation of the collision. Because of the lower stiffness of inter-vehicle crashes compared to crashes with a wall, the restitution coefficient for inter-vehicle crashes is smaller. The vehicle masses M_0 and M_{i} are chosen as equal for simplicity.

D. Motion Planner

In this section, we present the planner we use for the estimation of risk-sensitive trajectories. For this purpose, we vary the Ego vehicle trajectory according to a behavior model while trying to minimize the overall trajectory costs in terms of risk and benefits. In the simplest case, the behavior model is given by a short acceleration / deceleration interval followed by constant velocity driving.

To account for traveling benefits, we introduce two additional costs. On one side we incentivize the Ego vehicle to drive forward, using a cruising utility $q_{\text{cruise}}(t+s) = m_{\text{cruise}}|v_{\text{cruise}} - v_0(t+s)|$, which rewards the traveling progress with a predefined parameter m_{cruise}, a desired cruising velocity v_{cruise} and the ego velocity v_0. On the other side, we use a comfort utility $q_{\text{comf}}(t+s) = m_{\text{comf}}[a_0(t+s)]^2$, to punish high accelerations a_0 of the Ego vehicle.

Similar to the integrated risk in (4), the benefits are weighted by the survival probability:

$$Q_{\text{INT,cruise}}(t) = \int_0^\infty q_{\text{cruise/comf}}(t+s)\, S(t+s,t) ds. \tag{12}$$

The trade-off problem between all occurring risks and benefits is expressed by the overall costs C for the Ego vehicle with given trajectories of all traffic participants, which is equal to the sum of integrated risk (4) and benefits (12) along the Ego trajectory:

$$C(t) = Q_{\text{INT,cruise}}(t) + Q_{\text{INT,comf}}(t) + \sum_e R_{\text{INT,e}}(t). \tag{13}$$

Our planner uses the overall costs as feedback for the current scene and reduces them over time. We implement the desired behavior as an optimization problem where the best Ego vehicle acceleration $a_{0,\text{opt}}(t)$ is determined for the next time step (afterwards it is assumed for the prediction that the Ego vehicle continues driving with constant velocity). The planner relaxes critical situations by decreasing the costs, as far as its physical constraints (in our case minimal and maximal acceleration) hold.

$$a_{0,\text{opt}} = \min_{a_0(t) \in [a_{\min}, a_{\max}]} C(t) \tag{14}$$

Here we remark that since the overall costs $C(t)$ comprise also the entire future evolution of a scene, $C(t)$ also depends on the future states, and therefore on the Ego vehicle acceleration $a_{0,\text{opt}}$. In our case, we chose three base accelerations $a_0(t) \in \{a_{\min}, 0, a_{\max}\}$ to interpolate the costs in a quadratic fashion and solve for the minimum of this restricted one-dimensional quadratic problem, which can be easily solved.

A full and global numerical optimization would need iterative cost evaluations over the search space of all possible trajectories. To the contrary, the approach only evaluates the costs of only 3 different trajectories. In normal driving conditions, this suffices to find reasonable driving behaviors, since the cost $C(t)$ comprises the entire future risk of a scenario.

III. Simulations

The motion planner is able to plan in a dynamic environment by reducing the scene risk with the aid of the acceleration adjustment at the current time step. We demonstrate the behavior of our model on three different parallel lane scenarios. In the first scenario with purely longitudinal risk, we compare the trajectories of a car following scene on roadway with trajectories generated by the Intelligent Driver Model (IDM) [18]. In a second scenario, wo show the ability of lateral risk consideration, investigating overtaking behavior for varying lateral distance between both cars. In the last scenario, the Ego is positioned between two Other vehicles on the same lane meaning that our model has to incorporate more than one risk source to adapts its distance to the frontal vehicle depending on the distance to the rear-vehicle.

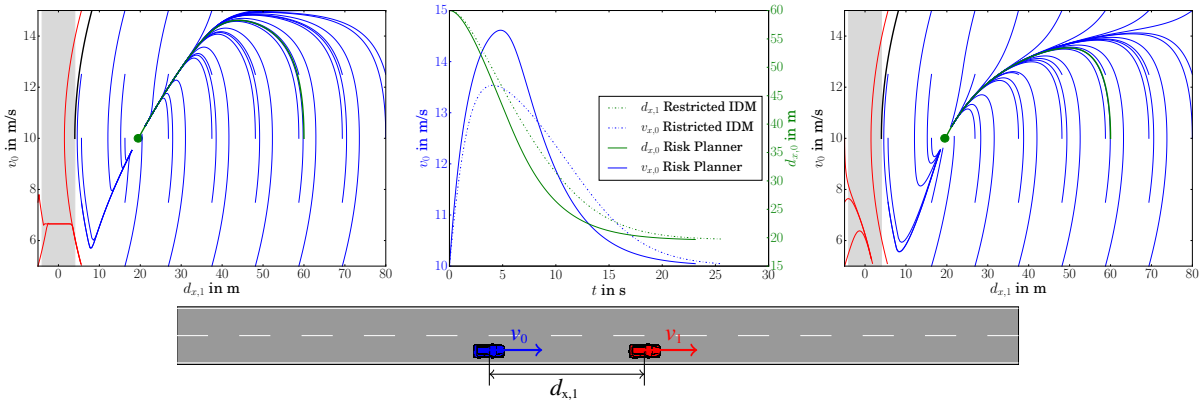

Figure 1: *Two-car following* scenario behavior with $\hat{v}_1 = 10\,\frac{m}{s}$. Bottom: Car following scenario with blue Ego vehicle behind a red Other vehicle. Left: Trajectories starting from different initial conditions (red trajectories lead to collision, blue trajectories converge into the green equilibrium point). Middle: Comparison of velocity and position curves over time for two chosen trajectories from the restricted IDM and our model. Right: Trajectories of an IDM model with restricted acceleration/deceleration. One can see that our models result in a similar stability behavior and trajectory curves.

A. *Two car following scenario*

In the two-car following scenario the Ego vehicle is driving behind another vehicle (see Fig. 1 below). The frontal car drives constantly with $\hat{v}_1 = 10\,\frac{m}{s}$. In the left of Fig. 1, we see the trajectories depending on the distance to the frontal vehicle and the ego velocity. One can see that the blue trajectories in the picture converge to a stationary distance, where the ego vehicle and the frontal vehicle have the same speed (green point). Contrarily, the red trajectories lead to an overlap of the two vehicle shapes and therefore to a crash (gray area). The black curve indicates the trajectory with the maximum possible deceleration that avoids a crash. We choose the well-known IDM and restrict its acceleration as in our model. The trajectories from the restricted IDM are depicted in the right of Fig. 1. We then compared our risk-avoiding trajectories with generated IDM trajectories starting at the same initial conditions (Fig. 1 middle). One can see that the qualitative behavior is very similar, with both models avoiding crashes whenever physically possible and both converging to a stable equilibrium without overshooting.

B. *Overtaking scenario*

To show the lateral influence on the longitudinal planning, we analyze an overtaking scenario, where one Other vehicle is driving on the neighbor lane and the Ego vehicle wants to pass this vehicle (see Fig. 2 bottom).

In scenarios where the lateral distance is sufficiently large and accordingly low collision risk, the Ego vehicle overtakes the Other without any influence on its driving behavior. For small lateral distance between both vehicles, the influence of the lateral collision risk dominates and a high amount of trajectories exhibits the stable following behavior from Fig. 1. For larger lateral distances the equilibrium point disappears and all shown trajectories produce an overtaking behavior (Fig. 2 left). In Fig. 2 (right), the equilibrium longitudinal distance as function of the lateral distance is shown for three Other vehicle speeds. We see that with increasing lateral distance, the longitudinal distance to frontal vehicle decreases smoothly up to the point when overtaking occurs. In the middle picture of Fig. 2 we show trajectories (velocity vs. time) with different initial velocities and lateral distances, which lead to a velocity decrease during the overtaking process. As a consequence, our model provides a smooth adaptation between a pure following behavior and free overtaking.

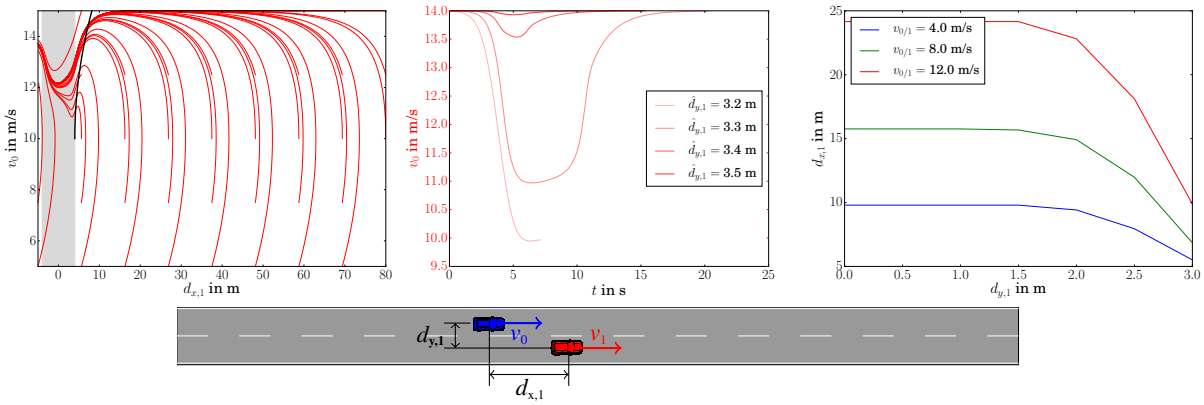

Figure 2: *Overtaking* scenario behavior with $\hat{v}_1 = 10\,\frac{m}{s}$. Bottom: Scenario with blue Ego vehicle and red Other vehicle on the neighboring lane. Left: Trajectories in the overtaking scenario starting from different initial conditions. Middle: Velocity and position curves for a set of chosen trajectories with different cruising velocity and lateral distance. Right: Longitudinal stability distance as function of the lateral distance to Other vehicle, for 3 different Other velocities. The lateral risk awareness of our model leads to a velocity-dependent distance keeping behavior together with appropriate smooth overtaking when the lateral distance gets sufficiently large.

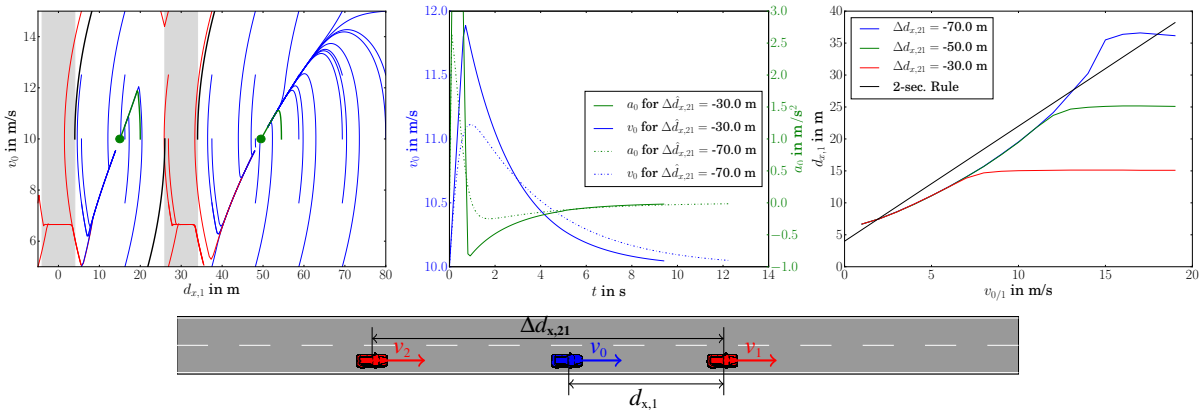

Figure 3: *In-between* scenario behavior with $\hat{v}_1 = 10\,\frac{m}{s}$. Bottom: Blue Ego vehicle in front of and behind red Other vehicles (gap distance between Others is $30\,m$). Left: Trajectories in the in-between scenario starting from different initial conditions (red trajectories lead to collision, blue trajectories converge into the green equilibrium points). Middle: Velocity and position curves for trajectories with equidistant initial Ego vehicle condition. Right: Resulting stationary distance to frontal vehicle as function of convoy velocity for three different gap sizes. One can see that our model can cope with more than one risk source. Furthermore, our microscopic driver model leads to an approximated two-seconds headway distance driving rule (black line).

C. *In-between positioning scenario*

In a dynamic environment like in a crowded traffic scenario, the Ego driver (see Fig. 3 bottom) might be influenced by more than a single other traffic participant. Our model allows to incorporate more than one risk source and therefore more than one traffic participant in a scene. The in-between positioning represents such a scenario, where the Ego vehicle is located between a frontal and a following vehicle, driving with constant speed $\hat{v}_1 = 10\,\frac{m}{s}$. In the left picture of Fig. 3, one can see that the rising part of the converging trajectories is steeper when the Ego vehicle is located between the Other cars and not only behind one car. The state curves are shown in Fig. 3 (middle) for an in-between scenario vs. a plain following scenario. The equilibrium distance depends on the convoy velocity and is limited by the presence of the rear-end vehicle as shown for 3 different gap sizes (see Fig. 3 right). For sufficiently large gap sizes, the rear cars influence disappears and the distance vs. velocity curve is the same as for the two car following scenario. It can also be seen that in this condition, an approximated two seconds headway distance rule appears (black line) [7], showing that our microscopic behavior model leads to macroscopic driving rules.

IV. Conclusion

In this paper, we presented a risk-aware driver model which can be used for trajectory prediction of other traffic participants in safety applications. We show that the model can incorporate arbitrary risks including several other traffic participants, and that it can be applied to longitudinal as well as lateral risks in different scenarios. For purely longitudinal scenarios, it results in smooth and plausible trajectories. We show up the smooth adaptation of the stability points depending on convoy velocity and lateral distance. In addition, it leads to a series of behaviors which are recommended and well known from heuristic safety driving rules, like the headway distance rule on motorways.

References

[1] X. Qian, F. Altché, P. Bender, C. Stiller, and A. de La Fortelle, "Optimal trajectory planning for autonomous driving integrating logical constraints: An miqp perspective," in *2016 IEEE 19th International Conference on Intelligent Transportation Systems (ITSC)*, pp. 205–210, Nov 2016.

[2] S. Luko, "Risk management principles and guidelines," *Quality Engineering*, vol. 25, Oct 2013.

[3] J. C. Hayward, "Near miss determination through use of a scale of danger," 1972.

[4] M. Schreier, V. Willert, and J. Adamy, "An integrated approach to maneuver-based trajectory prediction and criticality assessment in arbitrary road environments," *IEEE Transactions on Intelligent Transportation Systems*, vol. 17, no. 10, pp. 2751–2766, 2016.

[5] T. Puphal, M. Probst, Y. Li, Y. Sakamoto, and J. Eggert, "Optimization of velocity ramps with survival analysis for intersection merge-ins," in *2018 IEEE Intelligent Vehicles Symposium (IV)*, pp. 1704–1710, IEEE, 2018.

[6] J. Eggert, F. Damerow, and S. Klingelschmitt, "The foresighted driver model," in *2015 IEEE Intelligent Vehicles Symposium (IV)*, pp. 322–329, IEEE, 2015.

[7] G. Breyer, "Safe distance between vehicles," *Conference of European Directors of Roads*, April 2010.

[8] J. Eggert, "Predictive risk estimation for intelligent adas functions," in *17th International IEEE Conference on Intelligent Transportation Systems (ITSC)*, pp. 711–718, Oct 2014.

[9] C. Rodemerk, S. Habenicht, A. Weitzel, H. Winner, and T. Schmitt, "Development of a general criticality criterion for the risk estimation of driving situations and its application to a maneuver-based lane change assistance system," in *2012 IEEE Intelligent Vehicles Symposium*, pp. 264–269, IEEE, 2012.

[10] A. Lambert, D. Gruyer, G. S. Pierre, and A. N. Ndjeng, "Collision probability assessment for speed control," in *2008 11th International IEEE Conference on Intelligent Transportation Systems*, pp. 1043–1048, Oct 2008.

[11] N. Kaempchen, B. Schiele, and K. Dietmayer, "Situation assessment of an autonomous emergency brake for arbitrary vehicle-to-vehicle collision scenarios," *IEEE Transactions on Intelligent Transportation Systems*, vol. 10, no. 4, pp. 678–687, 2009.

[12] D. Althoff, *Safety assessment for motion planning in uncertain and dynamic environments*. PhD thesis, Technische Universität München, 2014.

[13] G. Xie, X. Zhang, H. Gao, L. Qian, J. Wang, and U. Ozguner, "Situational assessments based on uncertainty-risk awareness in complex traffic scenarios," *Sustainability*, vol. 9, no. 9, p. 1582, 2017.

[14] M. Müller, P. Nadarajan, M. Botsch, W. Utschick, D. Böhmländer, and S. Katzenbogen, "A statistical learning approach for estimating the reliability of crash severity predictions," in *2016 IEEE 19th International Conference on Intelligent Transportation Systems (ITSC)*, pp. 2199–2206, IEEE, 2016.

[15] W. Pawlus, H. Reza Karimi, and K. Robbersmyr, "Development of lumped-parameter mathematical models for a vehicle localized impact," *Journal of Mechanical Science and Technology*, vol. 25, pp. 1737–1747, July 2011.

[16] D. J. Gabauer and H. C. Gabler, "Comparison of delta-v and occupant impact velocity crash severity metrics using event data recorders," in *Annual Proceedings/Association for the Advancement of Automotive Medicine*, vol. 50, p. 57, Association for the Advancement of Automotive Medicine, 2006.

[17] H. Baum, T. Kranz, and U. Westerkamp, "Volkswirtschaftliche Kosten durch Straßenverkehrsunfälle in Deutschland," 2010.

[18] M. Treiber, A. Hennecke, and D. Helbing, "Congested traffic states in empirical observations and microscopic simulations," *Physical Review E*, vol. 62, pp. 1805–1824, Feb 2000.